

**Effect of Hybrid Composition and Volume Fraction on Microstructure and  
Microhardness of 7075 Aluminum Alloy via Friction Stir Processing**

by

Nur Nabila Najad binti Jaafar

25575

Dissertation submitted in partial fulfilment of

the requirements for the

Bachelor of Engineering (Hons)

(Mechanical)

JANUARY 2020

Universiti Teknologi PETRONAS

32610 Bandar Seri Iskandar

Perak Darul Ridzuan

CERTIFICATION OF APPROVAL

**Effect of Hybrid Composition and Volume Fraction on Microstructure and  
Microhardness of 7075 Aluminum Alloy via Friction Stir Processing**

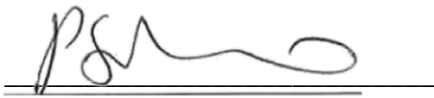
by

Nur Nabila Najad binti Jaafar

25575

A project dissertation submitted to the  
Mechanical Engineering Programme  
Universiti Teknologi PETRONAS  
In partial fulfilment of the requirement for the  
BACHELOR OF ENGINEERING (Hons)  
MECHANICAL

Approved by,



(AP. Dr. Srinivasa Rao Pedapati)

UNIVERSITI TEKNOLOGI PETRONAS

Bandar Seri Iskandar, Perak

January 2020

## CERTIFICATION OF ORIGINALITY

This is to certify that I am responsible for the work submitted in this project, that the original work is my own except as specified in the references and acknowledgements, and that the original work contained herein have not been undertaken or done by unspecified sources or person.



---

NUR NABILA NAJAD BINTI JAAFAR

## ABSTRACT

Most advanced engineering applications that require monolithic material structures with a broad variety of properties are hard to obtain. Composites in particular have enhanced substantial mechanical and tribological properties to fulfill the needs of the essential field of surface engineering. Friction stir processing (FSP) technology turns up as a promising technique in modifying microstructure and fabricating surface composites. Owing to their low density and high strength, aluminum alloys overtake steel alloys in various applications. Despite that, aluminum alloys are restricted under different loading conditions due to their weak surface properties. Hence, hybrid surface composites of aluminium matrix reinforced with Fly Ash (FA) and Graphite (Gr) are fabricated via FSP for this project. Experiments are conducted to study the relationship and find the optimum value of two parameters which are hybrid composition (60:40, 75:25, 90:10) and volume fraction (4%, 8%, 12%) of the reinforcement particles with regards to microhardness and microstructural characterization. Vicker's hardness technique and Optical microscopy are carried out for the composites performance evaluation. ANOVA analysis is also used to prove the significant contribution of volume percentage compared to hybrid ratio towards the composites hardness. Increment in volume percentage affected the increment of hardness up until 8% and showed rapid decrement afterwards. Hybrid ratio and hardness behaviour have nonlinear relationship where increase in fly ash content led to gradual increase in microhardness value. 4% to 8% and 84:16 to 90:10 are found to be the optimum reinforcements volume percentage and hybrid ratio for the surface composites, respectively. The presence and uniform distribution of the reinforcements particles are confirmed through the characterization of microstructures of the highest and lowest hardness samples. Vital and useful information of friction stir processing practical applications that could be used by the new researchers in order to fabricate more efficient surface composites are found.

## ACKNOWLEDGEMENT

بِسْمِ اللَّهِ الرَّحْمَنِ الرَّحِيمِ

Praise to Allah, The Most Gracious The Most Merciful. Blessings and peace be upon the leaders of the early and later generations, our Prophet Muhammad (Peace be upon him) and also upon his family and acquaintances.

First and foremost, I would like to praise Allah for giving me the patience, strength and spirit during the past 28 weeks in completing the Final Year Project required for last two semester in Universiti Teknologi PETRONAS. It has been such a wonderful voyage along these past few months of learning something new in the peak of being a graduate engineer.

Next, eternal and immense gratitude goes to my lovely and amazing parents, Mr. Jaafar bin Hamid and Mdm. Rizaida binti Idris, for their never-ending amounts of love, support and resilience in raising me since I was young and vulnerable, until I reach to this day, a grown up person. May their sacrifices and sincerity will be rewarded by Allah, The Most Magnificent.

I would also like to express my meaningful thanks to Assoc. Prof. Dr. Srinivasa Rao Pedapati, my serene supervisor for the close and effective surveillance and valuable knowledges shared with me. Besides, I am grateful and would give my biggest and deepest thanks to my incredible best friend and awesome people that have been great guidances and very helpful throughout my journey. They include Mr. Namdev Ashok Patil, fellow technologists as well as my final year colleagues.

Then, my keenest appreciation goes to Dr. Tamiru Alemu Lemma and Dr. Aklilu Tesfamichael Baheta, my bold FYP coordinators for all prominent managements, comprehensions and guidelines. Last but not least, a special recognition goes to both my outstanding examiners, Assoc. Prof. Dr. Zainal Ambri bin Abdul Karim and Assoc. Prof. Dr. Puteri Sri Melor binti Megat Yusoff for the wise evaluations and great commentary. Thank you.

# TABLE OF CONTENTS

<b>CERTIFICATION OF APPROVAL</b> .....	2
<b>CERTIFICATION OF ORIGINALITY</b> .....	3
<b>ABSTRACT</b> .....	4
<b>ACKNOWLEDGEMENT</b> .....	5
<b>CHAPTER 1: INTRODUCTION</b> .....	10
1.1 Background.....	10
1.2 Problem Statement.....	15
1.3 Objectives & Scope Of Study.....	16
<b>CHAPTER 2: LITERATURE REVIEW</b> .....	17
<b>CHAPTER 3: METHODOLOGY/PROJECT WORK</b> .....	24
3.1 Study Design.....	24
3.1.1 Preparation of Materials .....	24
3.1.2 Friction Stir Processing Application .....	27
3.1.3 Characterization & Mechanical Properties Evaluation.....	27
3.2 Sampling Specifications .....	28
3.2.1 Metal Matrix.....	28
3.2.2 Reinforcement Powders .....	29
3.3 Equipments and Consumables.....	30
3.3.1 Vertical Turret Milling machine .....	30
3.3.2 Turbula Mixer .....	30
3.3.3 Weighing Balance .....	31
3.3.4 Friction Stir Welding machine .....	31
3.3.5 Electrical Discharge Machine .....	32
3.3.6 Automatic Mounting Press.....	32
3.3.7 Grinder Polisher .....	33
3.3.8 Microhardness Testing Machine .....	33
3.3.9 Optical Microscope .....	34
3.4 Project Activities and Milestone.....	35
<b>CHAPTER 4: RESULTS AND DISCUSSION</b> .....	36
4.1 Microhardness .....	36

4.1.1 Data Tabulation .....	36
4.1.2 ANOVA Analysis.....	38
4.1.3 Contour Graph .....	41
4.2 Microstructure .....	42
4.2.1 Data Collections & Analysis of Run 4 Composites...42	
4.2.2 Data Collections & Analysis of Run 8 Composites....45	
<b>CHAPTER 5: CONCLUSION AND RECOMMENDATION.....</b>	<b>48</b>
<b>REFERENCES .....</b>	<b>50</b>

## LIST OF FIGURES

Figure 1.1	Friction Stir Processing Schematic Diagram	11
Figure 1.2	Fly Ash	14
Figure 1.3	Graphite	14
Figure 2.1	Friction Stir Processing Schematic Diagram	21
Figure 2.2	Microhardness Testing	23
Figure 3.1	Holes Pattern	25
Figure 3.2	Flowchart	25
Figure 3.3	Experimental Process Flow	26
Figure 3.4	7075 Aluminium Plate	29
Figure 3.5	Vertical Turret Milling Machine	30
Figure 3.6	End mill	30
Figure 3.7	Turbula Mixer and Glass Jar	30
Figure 3.8	Weighing Balance	31
Figure 3.9	Containers	31
Figure 3.10	FSW Machine	31
Figure 3.11	Pin Profile	31
Figure 3.12	Electro Discharge Machining	32
Figure 3.13	Mounting Press Machine	32
Figure 3.14	Phenolics Granule	32
Figure 3.15	Grinder Polisher	33
Figure 3.16	Diamond Paste	33
Figure 3.17	Vicker's Microhardness Testing Machine	33
Figure 3.18	Optical Microscope	34
Figure 4.1	Graph of Volume Percentage at 75:25 Hybrid Ratio (vol%) vs Microhardness (HV).	40
Figure 4.2	Graph of Hybrid Ratio at 8% Volume Percentage (HR) vs Microhardness (HV)	41
Figure 4.3	Contour Graph of Hybrid Ratio and Volume Percentage vs Microhardness	42
Figure 4.4	50X Magnification of Run 4 Composites	43
Figure 4.5	100X Magnification of Run 4 Composites	43
Figure 4.6	500X Magnification of Run 4 Composites	44
Figure 4.7	50X Magnification of Run 8 Composites	45

Figure 4.8	100X Magnification of Run 8 Composite	46
Figure 4.9	500X Magnification of Run 8 Composites	46

## **LIST OF TABLES**

Table 1.1	Composition, Mechanical Properties, and Typical Applications for Several Common Aluminum Alloys	13
Table 4.1	Run 1 Hardness Test Results	36
Table 4.2	Run 2 Hardness Test Results	36
Table 4.3	Run 3 Hardness Test Results	36
Table 4.4	Run 4 Hardness Test Results	37
Table 4.5	Run 5 Hardness Test Results	37
Table 4.6	Run 6 Hardness Test Results	37
Table 4.7	Run 7 Hardness Test Results	37
Table 4.8	Run 8 Hardness Test Results	37
Table 4.9	Run 9 Hardness Test Results	37
Table 4.10	Run 10 Hardness Test Results	38
Table 4.11	Hardness Test Results Summary	38
Table 4.12	ANOVA Analysis Input	38
Table 4.13	ANOVA Analysis Summary	39

# CHAPTER 1

## INTRODUCTION

### 1.1 Background

The choice of a material with appropriate attributes and quality is one of the most critical aspects of many industrial applications. In industries such as aerospace and automotive, the selection of an alloy requiring requirements such as proper grain strength and uniformity is crucial. Metal Matrix Composites (MMCs); an engineered material made by combining two or more dissimilar materials (at least one of which is a metal), is produced in order to acquire optimized material properties. For instance, one way to boost the microhardness of aluminum alloys while maintaining their lightweight is by producing the MMC using extremely high-resistance materials like beryllium and graphene.

Today, composite construction is the most indispensable advance in material history. Due to its ability to enhance the mechanical and physical properties of conventional fiber reinforced composites, nanoparticles are gaining more attention in the integrated community. The main objectives of introducing new material processing methods may lead to the need to build a material with fine grain size, sufficient strength and ductility while saving time and cost. There are several manufacturing methods for materials, such as Equal Channel Angular Extrusion (ECAE) and FSP, where both have achieved their desired objectives.

Friction Stir Processing (FSP) has successfully developed as an alternative method of fabricating MMC. Friction stir processing is a novel technique of solid-state processing with low heat input operations and will possibly produce samples with great mechanical properties. It is a new technique evolved by Mishra et al. utilizes the Friction Stir Welding (FSW) which then makes FSP to have similar process principles with FSW. Instead of joining samples together, FSP differs from FSW by inserting the rotating tool in a monolithic specimen. Heating is localized and produced by friction between the tool of the equipment and specimen, with additional adiabatic metal deformation heating. The movement of material from the

front of the pin to the back of the pin produced a processed zone. A schematic illustration of FSP is shown as in Figure 1.1.

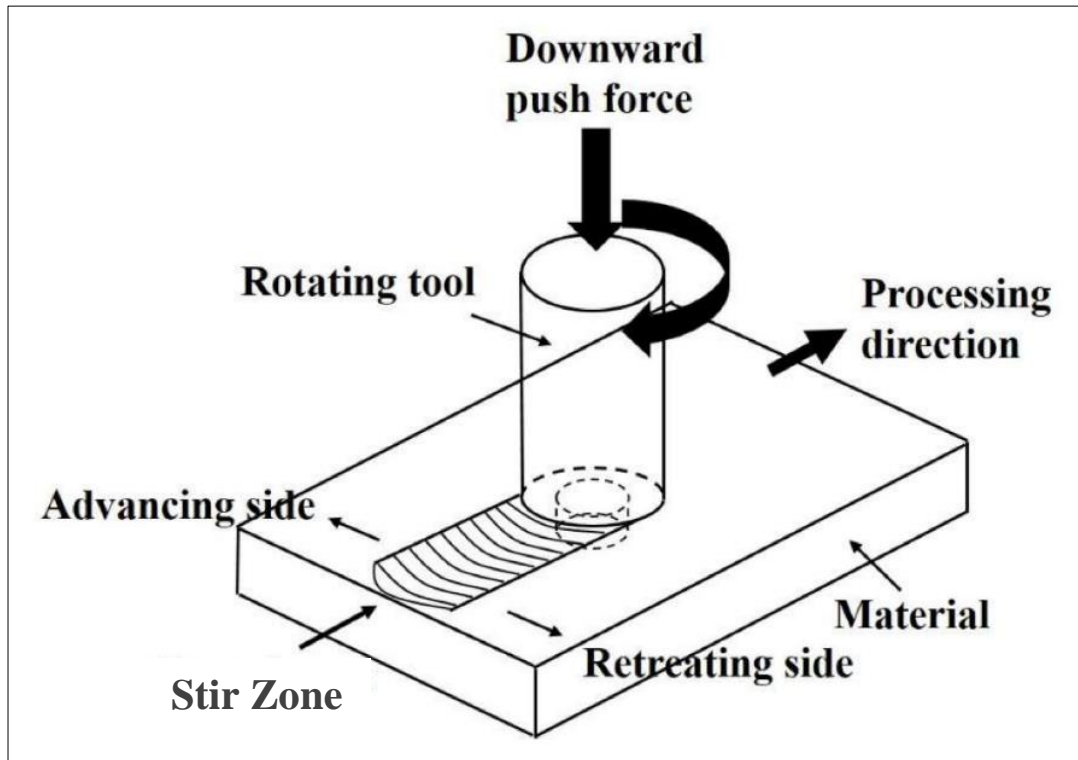


FIGURE 1.1 : Friction Stir Processing Schematic Diagram

Furthermore, FSP technology is primarily used for microstructure alteration in layers near to the surface of processed metal components. This process may produce better grain structure, integrated substrate, and alloying with specific components as well as improve welded joints quality. Moreover, this method used to enhance the conventional methods for materials processing such as the Rockwell and powder metallurgy approaches [1]. To achieve superplasticity, particularly high strain rate superplasticity (HSRS), FSP can be implemented in aluminum alloy which leads to very fine equiaxed grain microstructure [2]. Some preferences or characteristics of FSP which make it outstanding from the other metalworking methods are listed as per below [3]:

- It can be done in a single pass, with microstructural purification, homogenisation and also densification [4]
- By tuning the FSP parameters and enabling the cooling or heating, the microstructure behavior analysis and the mechanical properties of the processed zone can be carried out.
- Changing the length of the rotational pin tool allows for observation on the depth of the processed region. This capability illustrates FSP's stability in supporting the different depth ranges from tens of millimetres (mm) to hundred micrometres ( $\mu\text{m}$ ).
- FSP is a green and energy efficient method because the input heat generation cycle is accomplished by means of friction and plastic deformation. Plus, the FSP process does not create any harmful gas or radiation and noise.
- Employing FSP method can keep the size and shape of the material intact and will not alter them.
- FSP is a fair approach because it does not require any special equipment or facilities. It can be carried out by using any machines available, such as conventional milling.

The study of FSP impacts on wrought alloy is carried out on Aluminum 7075 (AA 7075-T651), which is used as as the matrix element while the second phase material consists of a mixture of Fly Ash and Graphite act as composites reinforcements. 7075 aluminum alloy consists of 5.6 Zinc (Zn), 2.5 Magnesium (Mg), 1.6 Copper (Cu), and 0.23 Chromium (Cr) by weight proportion (wt %). This process developed Aluminum Matrix Composites (AMCs) which is one of the MMCs using selected materials. The key reasons for having aluminum 7075-based composite are that it attracts considerable attention due to aluminum and its alloy attributes that are fairly light in weight, ideal for heat treatment, high resistance to pressure, low yield strength, high ductility, high resistance to corrosion, moderate casting temperature, strong heat and electricity conductor and are 100% recyclable. Aluminum has a high wear rate and low hardness, in spite of all these positive qualities. For the compositions, properties and applications of some wrought and cast aluminum alloys, see Table 1.1.

TABLE 1.1 : Composition, Mechanical Properties, and Typical Applications for Several Common Aluminum Alloys

Aluminum Association Number	UNS Number	Composition (wt%) <sup>a</sup>	Condition (Temper Designation)	Mechanical Properties			Typical Applications/ Characteristics
				Tensile Strength [MPa (ksi)]	Yield Strength [MPa (ksi)]	Ductility [%EL in 50 mm (2 in.)]	
<b>Wrought, Nonheat-Treatable Alloys</b>							
1100	A91100	0.12 Cu	Annealed (O)	90 (13)	35 (5)	35–45	Food/chemical handling and storage equipment, heat exchangers, light reflectors
3003	A93003	0.12 Cu, 1.2 Mn, 0.1 Zn	Annealed (O)	110 (16)	40 (6)	30–40	Cooking utensils, pressure vessels and piping
5052	A95052	2.5 Mg, 0.25 Cr	Strain hardened (H32)	230 (33)	195 (28)	12–18	Aircraft fuel and oil lines, fuel tanks, appliances, rivets, and wire
<b>Wrought, Heat-Treatable Alloys</b>							
2024	A92024	4.4 Cu, 1.5 Mg, 0.6 Mn	Heat-treated (T4)	470 (68)	325 (47)	20	Aircraft structures, rivets, truck wheels, screw machine products
6061	A96061	1.0 Mg, 0.6 Si, 0.30 Cu, 0.20 Cr	Heat-treated (T4)	240 (35)	145 (21)	22–25	Trucks, canoes, railroad cars, furniture, pipelines
7075	A97075	5.6 Zn, 2.5 Mg, 1.6 Cu, 0.23 Cr	Heat-treated (T6)	570 (83)	505 (73)	11	Aircraft structural parts and other highly stressed applications
<b>Cast, Heat-Treatable Alloys</b>							
295.0	A02950	4.5 Cu, 1.1 Si	Heat-treated (T4)	221 (32)	110 (16)	8.5	Flywheel and rear-axle housings, bus and aircraft wheels, crankcases
356.0	A03560	7.0 Si, 0.3 Mg	Heat-treated (T6)	228 (33)	164 (24)	3.5	Aircraft pump parts, automotive transmission cases, water-cooled cylinder blocks
<b>Aluminum-Lithium Alloys</b>							
2090	—	2.7 Cu, 0.25 Mg, 2.25 Li, 0.12 Zr	Heat-treated, cold-worked (T83)	455 (66)	455 (66)	5	Aircraft structures and cryogenic tankage structures
8090	—	1.3 Cu, 0.95 Mg, 2.0 Li, 0.1 Zr	Heat-treated, cold-worked (T651)	465 (67)	360 (52)	—	Aircraft structures that must be highly damage tolerant

<sup>a</sup>The balance of the composition is aluminum.

Source: Adapted from *ASM Handbook*, Vol. 2, *Properties and Selection: Nonferrous Alloys and Special-Purpose Materials*, 1990. Reprinted by permission of ASM International, Materials Park, OH.

Taking into account the FSP's enhancement of mechanical and microstructural properties, the aluminum alloy is strengthened with a hard and porous dispersed or second phase. In this case, Fly Ash and Graphite powders as shown in Figures 1.2 and 1.3 are used due to their high strength, high hardness and

less density properties. In addition, the composite used in the investigation is a hybrid composite which consists of two or more particle-shaped reinforcements. It is likely that the combination of particle reinforcement materials will have significantly better properties and that the impact of failure where it is not as disastrous as with single-particle composites. Moreover, they must be integrated in the matrix to slightly surpass the values of the strength-density and modulus-weight ratios while retaining good efficiency at a reduced cost, as fly ash is the agro waste. The recently manufactured material has great tribological and mechanical properties and it has been found that often hybrid composites (multi-reinforcements) demonstrate greater qualities than single composites of reinforcement, pure aluminum and their alloys regardless of the aluminum matrix composites manufacturing process.



FIGURE 1.2 : Fly Ash



FIGURE 1.3 : Graphite

The FSP process's principal technical parameters are rotational or rotating speed, transverse or travelling speed, number of passes and tool geometries that include probe length, probe diameter and shape, shoulder diameter and shape. In addition, alloying content, tool penetration depth, and tilt angle can have major effects on surface composite layer development. Experiments are carried out to analyze the effect of modifications on the microstructure and strength of aluminum alloy composites from two process variables which are hybrid composition and volume fraction of reinforcement particles. Investigation is performed with fixed parameters such as geometry of the tool, rotational speed, transverse speed, and number of passes.

## **1.2 Problem Statement**

Manufacturing sectors aim on the one hand to enhance the operational properties and implement eco-friendly materials in manufactured products, and on the other hand to reduce the mass of a product. Those demands led to surface layers production which represent required functional properties. The use of aluminium alloys in automotive applications are steadily growing because of their lightweight and excellent strength-to-weight ratio. Despite having great properties, aluminium alloy lacks of surface properties that limit their broader applications. Hybrid surface composites with adaption of agrowastes reinforcements such as fly ash are needed to fulfill the industrial needs. Due to special microstructure characteristics produced by friction stir processing technology, microhardness behaviour is believed to have a significant impact on the mechanical properties of aluminium alloy. Thus, it is a necessity to study the hardness behaviour of aluminium FSPed samples under various processing parameters including hybrid particles composition and volume fraction of material's reinforcements.

### **1.3 Objectives & Scope Of Study**

The proposed work aims at incorporating the process parameters, which are hybrid composition and volume fraction of particle reinforcement. The implemented corporation is to find the relationship among them, on the microstructure and hardness behaviour of friction stir processing of 7075 aluminium alloy. The proposed investigation is carried out to attain the following objectives:

- To improve the surface properties of 7075 (T651) aluminum alloy by adding reinforcements particles of fly ash and graphite
- To study the effect and observe optimum ratio of hybrid composition (FA – Gr particles ratio) on the composites by analysing the trend line of microhardness value and microstructural characterization of AA 7075-T651
- To obtain the optimum value from various reinforcements' volume percentage by conducting trend line for hardness behaviour analysis and investigate the impacts on microstructure of the composites samples.

#### ***Scope of study***

- This research is supplemented by laboratory work to produce hybrid aluminum matrix composites with fly ash and graphite reinforcements using Friction Stir Processing
- The research focused on investigating the characterisation of microstructures and mechanical properties such as microhardness of FSPed 7075 aluminium base alloy.

## CHAPTER 2

### LITERATURE REVIEW AND THEORY

Prabhakar et al. [5] illustrated that composites are a class of composite materials which offer many advantages as structural materials. AMC is classified as metal matrix composites (MMCs), a composite material group in which any metal is being used as a matrix material distributed with an effective secondary phase or fiber or particle reinforcement. Smith & Hashemi [6] have also explained that Matrix is a durable continuous substance that keeps the dispersing process stiff and brittle. The composite properties rely on the phases and the composition, size and shape of the constituents. Surface MMCs play a vital role in providing a strong and high wear-resistant surface without disrupting core properties.

According to Nelson et al. [7] and Callister, Jr. & Rethwisch [8], Aluminium matrix composites (AMCs) are outstanding candidates that is extremely useful for applications in aircraft industries owing to the excellent strength-to-density ratio, high ductility of the matrix and the high strength of hard reinforcing phases. One of the reasons is because aluminum has an FCC (face-centered cubic) crystal structure where its ductility can be retained even at very low temperatures. Besides that, the use of aluminum alloys in automotive applications is gradually increasing, owing to their low density. These trends resulted from improvement in fuel efficiency that is gained from the vehicles' weight reduction. Unfortunately, even possessing attractive properties, aluminum alloy has low wear resistance. While AMCs possess many attractive properties, integrating non-deformable ceramic reinforcements into the aluminum matrix results in a substantial loss of ductility and toughness. The surface properties determine the life span of the many components. The reinforcement of the surface layer of components with ceramic particles would thus allow the material of the internal matrix to maintain the original composition and to obtain greater toughness. This surface layer is generally called a surface composite.

Next, Davis [9] reviewed that based on their special qualities such as good mechanical qualities, excellent performance, durable and long-lasting, the use of aluminum-based composite grows day by day in the entire manufacturing sector. Very few structural metals or alloys have ultimate ratios of strength to density over 1,000,000 to 1. The typical structural metals, magnesium, aluminum, and steel module-to-density ratios are all approximately 100,000,000 to 1. Thirumoorthy et al. [10] also highlighted that in order to achieve the desired structural shapes materials such as graphite, titanium carbide, boron, fly ash, silicon carbide, beryllium, aluminium oxide, boron nitride, and even fine steel wire which attained properties that far exceed the strength and modulus to weight ratios, need to be incorporated in the matrix. Much work has subsequently been carried out in aluminum composite material with the introduction of particulate reinforcement dependent on carbides. Yet the manufacturing industries are searching for the best products in the present competitive market, producing simple nature and environmentally sustainable based materials. It is observed that there is massive work gap for development of excellent properties and eco-friendly materials.

Add Thirumoorthy et al. [10], new breed of hybrid composites has been developed which require the use of agro- and industrial waste derivatives. Interestingly, compared with the unreinforced alloy, they have shown better performance. One of the examples of commonly used agro waste is fly ash. Referring to Basham et al. [11], Fly ash is the by-product of the burning of pulverized coal in power plants. In the combustion chamber, mineral impurities in the coal (clay, feldspar, quartz, and shale) ignite in suspension and float with exhaust gasses. It cools and solidifies as the fused material develops in spherical glassy particles which are called fly ash. This is absorbed from the exhaust gas by electrostatic precipitators or bag filters. The fine powder resembles portland cement, but is chemically distinct. Nevertheless, there is still a need to research the degree of improvement of hybrid AMCs, which includes fly ash over the single reinforced AMC containing synthetic reinforcement. Nonetheless, hybrid AMCs combined with agro-waste derivatives demonstrated that high performance levels in AMCs can be sustained at minimal cost of production, even if conventional reinforcement with agro-waste is substituted by about 50%.

Tangarasu et al. [12] stated that FSP is used to examine the effect on microstructure, mechanical and sliding wear behavior of Titanium Carbide (TiC) particles, their volume fraction. Results showed that TiC particles had a major impact on the composite field, dispersion, matrix grain size, microhardness, UTS, and sliding wear function. Besides that, the distribution of TiC particles was fairly homogenous in the composite and AMCs exhibited a reduction in the average grain size. Not only that, TiC particles enhanced the wear resistance of the AMC. In some discoveries, increasing the graphite content in the aluminum matrix leads to massive improvements in ductility, UTS, compressive strength and Young's modulus, however a loss in hardness.

Prabhakar et al. [5] have wrote on Fly ash powder that was dispersed by groove filling method. The FSP works with varying speeds and feed rates. Better surface mixtures of Al 5083-fly ash with enhanced mechanical properties can be produced. As a result, microhardness was found to increase the FSPed Al 5083 and composite likely due to grain alteration, decreased secondary phase, and the fly ash occupancy in the matrix. The rate of corrosion had been estimated as decreased after FSP. Akinlabi et al. [13] also found the same results where microhardness profiling of the treated samples showed an improved hardness value relative to the parent material when integrating the TiC particle operation. Based on the set of processing parameters considered in the study, a moderate rotational speed of 1200 rpm and a minimum speed of 100 mm / min made the surface composite layer with excellent wear resistance property, which can be considered as the optimal parameter window. Besides, another researchers discovered that with the introduction of SiC and fly ash in Al2024 alloy, the percentage of elongation of hybrid MMCs is substantially reduced.

Nelson et al. [7] highlighted that surface composites exhibit enhanced characteristics of composites on the surface while retaining properties of the base material. Sharma et al. [14] expressed the same opinion and also explained that surface composites are produced using traditional liquid phase processing methods such as plasma spray, high-energy laser beam, cast sinter and irradiation by electron beams. Regardless of the high processing temperature, decomposition of ceramic particles is difficult to prevent. Multiple manufacturing methods are available for the manufacture of nano-sized (or micro-size) particle/metal composites, often based on

casting or powder metallurgy. Nevertheless, uniform dispersion of nano-sized particles into molten metal can be incredibly hard. A typical casting flaw which is micro-level porosity, can also be detrimental to the manufacture of micro-level geometry. Although powder metallurgy based techniques are effective in producing MMC successfully, usually the manufacturing process is very time consuming and may not be cost-effective in the processing of bulk composites. Conventional aluminum alloy fusion welding also gives the effect of porosity and warm cracks within the welded joint. It also impairs the mechanical properties as well as the resistance to corrosion. Hence, It would be extremely useful if a solid-state process that prevents bulk melting of the base materials, hot cracking and porosity can be created and implemented for aluminum alloy modifications.

The modification of aluminium alloy components is also still limited. Fortunately, Mishra and her colleagues developed a technique for microstructural modification of materials namely Friction Stir Processing (FSP). FSP technology is a great representation of fusion technology (FSW), that can be applied for other applications such as reconstruction as well as reducing the problems faced by other manufacturing technology and can also be very efficient for MMC manufacturing. Mishra et al. [1] and Sarmadi et al. [15] explained that friction stir processing is a technique of alteration of the surface in solid state using the same approach as friction stir welding (FSW); a solid state joining technique developed in the United Kingdom by The Welding Institute (TWI) and initially applied to the development of aluminum substrate surface composite. In FSW, a non-consumable rotating tool with a pin and a shoulder is inserted in adjoining sheets or plates into the joint gap and passed along the joint line causing the joining of plates.

Mishra et al. [1] and Sharma et al. [14] described that during FSP, a rotating tool is inserted into a substrate where a pin is thrust into the modified material with the rotating tool shoulder connected to the base metals. The tool performs two main purposes, namely heating and deformation of workpiece material. The shoulder movement, under the impact of the load applied, heats the metal around the altered area, as the pin automatically stirs the material that reverses the modified direction. This makes the frictional heat produced by the tool soften the material. Then, the pin's rotating action caused metal to flow from each section and to build the altered

field. As a result, a rigid plastic defective zone or stirring zone containing very fine grains is produced. The microstructure that developed during FSP is influenced by the material movement, deformation of plastics, high temperature, and features a central stirring zone surrounded by a thermally mechanically affected zone (TMAZ) and a heat affected zone (HAZ) during the FSP process. The deformed material is moved back to the forward side or advancing side (AS) from the back or retreating side (RS) of the tool, which is fabricated with the tool shoulder where this results in solid-state content modification. For the schematic representation of the FSP see Figure 2.1.

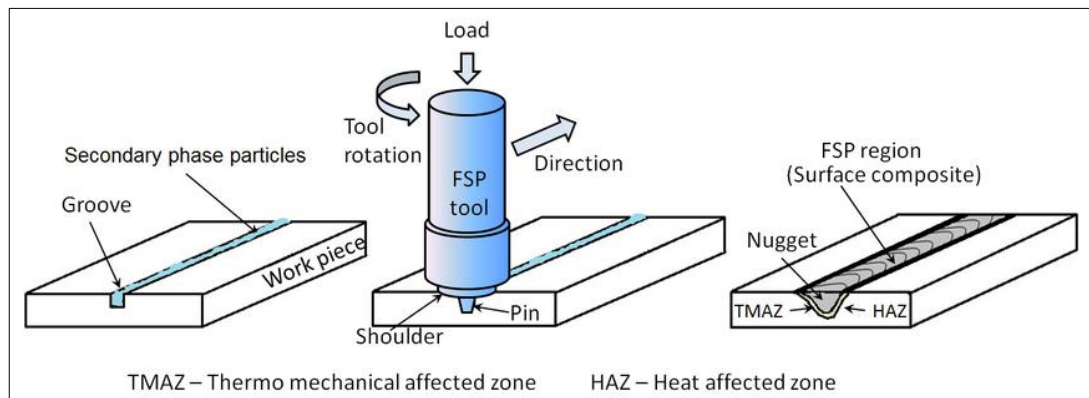


FIGURE 2.1 : Friction Stir Processing Schematic Diagram

Gan et al. [16] stated that FSP shares the same facilities with FSW and could have better properties compared with traditional processing technologies. FSP, for example, demonstrates its effectiveness in the homogenisation of aluminum alloys developed by powder metallurgy, effectively eliminates casting defects and separates or dissolves particles in the second phase and leads to major changes in properties such as the production of ultrafine grained substances. Weglowski [17] also acknowledged that FSP has many benefits over other technologies, and it is important to note that it is a green technology that does not generate smoke and dust and does not require the use of skilled welders but only operators of equipment. This updated technology is a relatively fresh and daunting process for development of microstructural, refinement and also enhancement of property.

Hirata et al. [18] have investigated the microstructure that was evolved into fine grains by the dynamic recrystallization during FSP. They also investigated the relationship between grain size advection-halogen parameter. We demonstrated that in all manufacturing conditions, the FSP-ed pure aluminum grain sizes were smaller than 10  $\mu\text{m}$ , and there was no major variation between the grain size. The Al-Mg alloy grain size went down to 0.27  $\mu\text{m}$ . Due to the high-temperature deformation process, FSP technique allows deformation to attain microstructure with certain minimum grain sizes, with adequate Z-value.

Sharma et al. [14] and Namdev et al. [19] explained the effect of reinforcement particles on grain refining that may be correlated with Zener pinning, which is the movement of grain boundaries that migrate due to recrystallization and grain growth that may be pinched by small second phase particles. Zener limiting grain size ( $d_z$ ) can be expressed as per below.

$$d_z = \frac{4r}{3V_f} \quad \text{where } r : \text{radius of second phase particles}$$

$$V_f : \text{Volume fraction of second phase particles}$$

Particulate enhancements can limit abnormal grain production, reduce stir zone area, and thus enhance material hardness by up to three times as compared to base alloy.

Additionally, tensile strength, yield strength and hardness are improved by raising the area fraction of matrix strengthening. Ikumapayi et al. [20] have explained the calculations of the proportion of the groove to the second phase materials as shown in equations below:

$$\text{Volume of fraction} = \frac{\text{Area of groove}}{\text{Projected area of tool pin}} \times 100$$

$$\text{Area of the groove} = \text{Groove width} \times \text{Groove depth}$$

$$\text{Projected area of the tool pin} = \text{pin diameter} \times \text{pin length}$$

Shan [21] explained that microhardness can artificially display the elasticity, plasticity and strength of materials. When measuring the hardness distribution in the weld, the result showed that the softening occurs in the particular area. This is

because, after melting and solidifying, the strengthening effect of the base metal is lost due to cold work. The depth of the weld is measured near the microhardness axis of the zone. It was found that the average microhardness at the bottom of the weld was the highest, the average microhardness above the weld was medium, and the average microhardness at the bottom of the weld was the lowest. This is in line with the principle that the grain size changes in the direction of the weld, which shows that the microhardness of the weld increases as the grain size decreases. In microhardness testing, an indentation is performed in the form of a diamond indenter by applying a load  $P$  as in Figure 2.2. Using a calibrated optical microscope, the resulting indentation size,  $d$  is measured, and the hardness is determined as the average pressure applied below the indenter.

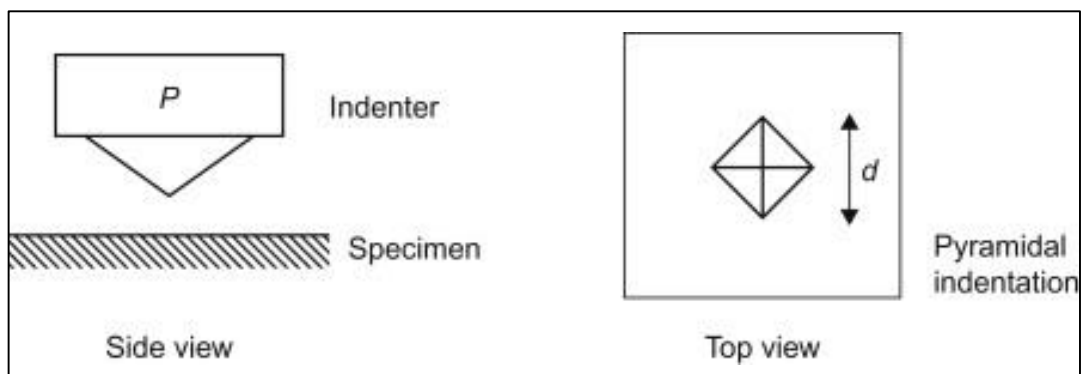


FIGURE 2.2 : Microhardness Testing

## **CHAPTER 3**

### **METHODOLOGY / PROJECT WORK**

#### **3.1 Study Design**

Experimental project method is divided into 3 parts, which are material preparation, application of Friction Stir processing, and characterization of composites comprising of evaluation of microstructural and mechanical properties. The process flow for the whole experimental project are as shown in Figure 3.2 and 3.3.

##### **3.1.1 Preparation of Materials**

First of all, 3 plates of 7075 (T651) aluminum alloy are prepared as the matrix with dimensions of 100 mm wide, 150 mm long and 6 mm thick. For the particle reinforcements, Fly Ash and Graphite powders are weighed for 1500 g in total by using weighing scale for each ratio of 60:40, 75:25 and 90:10 accordingly and kept in labelled containers. For the ratio, the maximum of Gr content is limited to 40% due to the very high thermal conductivity where more than 40% Gr in a sample will cause the composite band's tattered. Then, every mixture of hybrid composition are put in a glass jar and blended together by using Turbula Mixer for 4 hours to achieve an even particles distribution. Next, the plates are marked manually with 3 straight lines of 5 mm, 7 mm and 9 mm inter-cavity spacing (ICS) representing 12%, 8% and 4% of hybrid volume percentage. 3 mm depth with 3 mm diameter holes are then drilled on the surface of the plates with 1800 rpm spindle speed. The technique utilized is the Surface Blind Holes Method which refers to an approach that produces a hole by reaming, drilling, or milling to a defined depth without breaking to the other side of the workpiece. This method is accomplished by using Vertical Milling machine. The pattern of holes is one straight line and can be seen as per Figure 3.1. The plates then cleaned and followed by manual compaction process which is filling the cavity with Fly Ash-Graphite particles that comply the hybrid composition ratio by using allen key that fit the 3 mm holes.

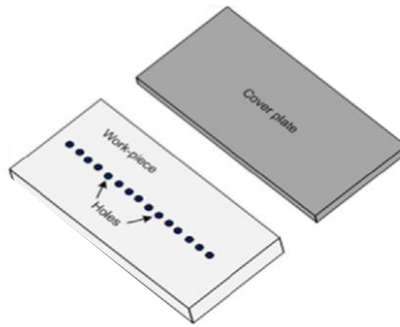


FIGURE 3.1 : Holes Pattern

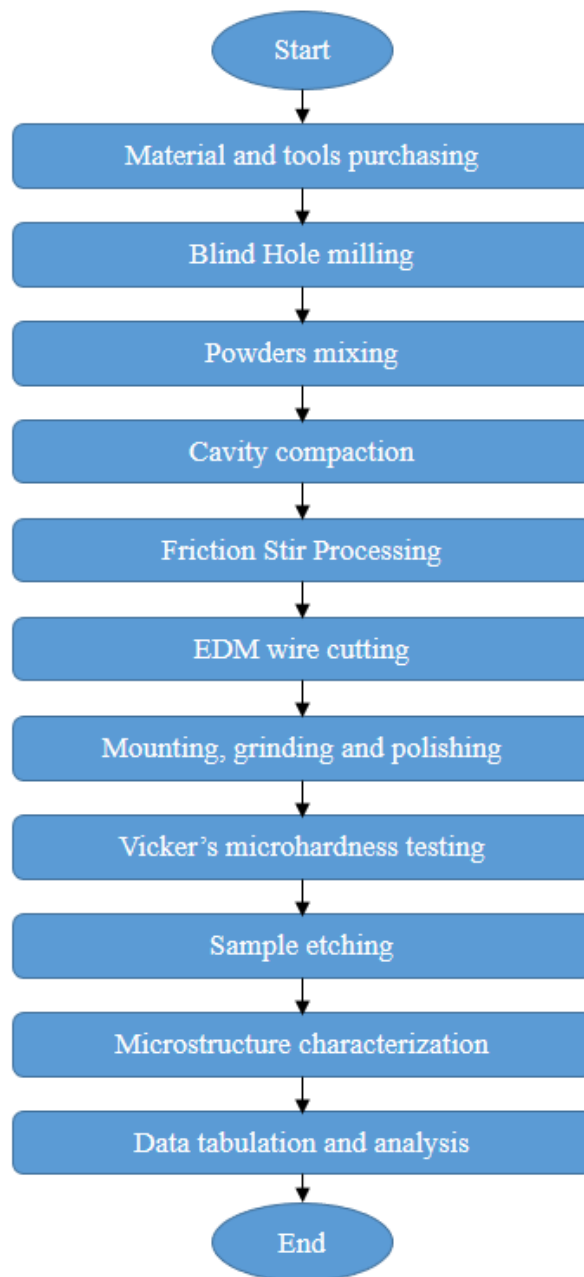


FIGURE 3.2 : Flowchart

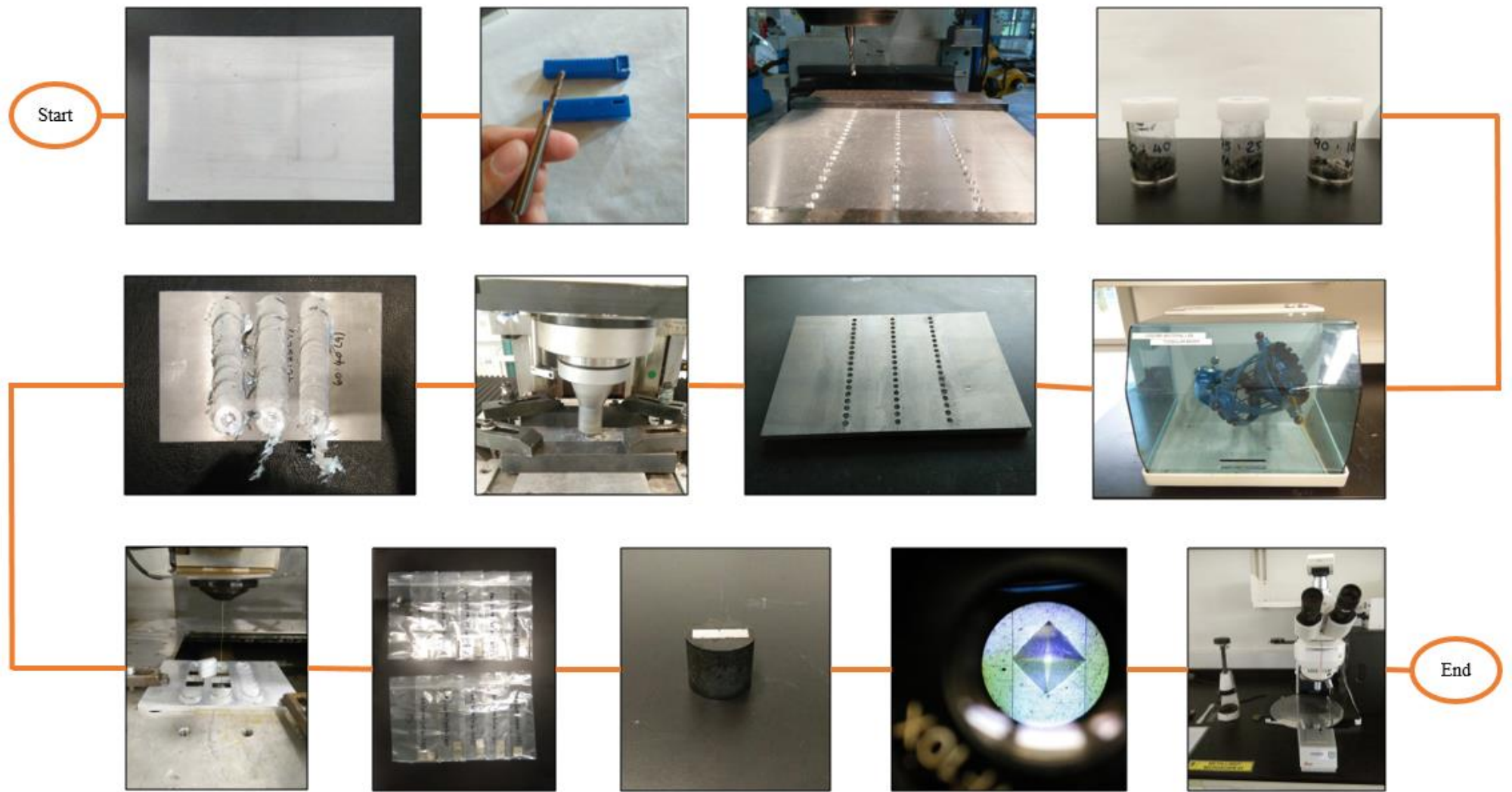


FIGURE 3.3 : Experimental Process Flow

### **3.1.2 Friction Stir Processing application**

FSP is a method that applies a probe (pin) tacking tool to the workpiece with essential parameters such as rotation rate of the tool, traverse speed and spindle angle of the tool (angle between spindle and workpiece normal). The tool with profile of straight cylindrical that made of H13 steel is used and essentially consists of a shoulder and a pin. Best tool shoulder to probe diameter ratio is applied in this experiment which is more than 3. Before welding process is executed on the plates, they are labelled accordingly after the compaction process. An optimum rotational speed,  $\omega$  of 1000 rpm and traverse speed,  $v$  of 40 mm/min are applied for the FSP. Several set up steps have been done including fixing a downward force of 10 kN with  $2^\circ$  tool angle and 5 mm plunge depth. The plate is then processed and subjected to only a single pass FSP. The FSPed plates are then cut into 9 squared shape thin slices of stir zone and 1 as-cast with dimensions of 20 mm  $\times$  20 mm  $\times$  6 mm using wire cut electrical discharge machining (EDM).

### **3.1.3 Characterization and Mechanical Properties Evaluation**

Composites are prepared properly for the accuracy of testing. Composites undergone mounting, grinding and polishing processes. For every samples, the surfaces that will be evaluated are coated with release agent and then mounted with Phenolics powders for about 15 minutes. Next, samples are grinded using Silicon Carbide (SiC) papers with grit of 400, 800 and 1200 for about 5 minutes each with water as the lubricant. The samples are held perpendicular to the grinder motion and parallel for the next SiC paper with different grit size and repetition of steps are implemented for the following grit of grinding papers. Later, samples undergone polishing process on a velvet cloth that is poured with MetaDi fluid for lubrication. Diamond Polishing Compound of 6  $\mu\text{m}$  and 3  $\mu\text{m}$  are then put consecutively onto the surface of the samples for about 5 minutes each. Technique of perpendicular and parallel to the motion of polisher are applied until the samples turned into mirror finish.

The samples are then ready for the evaluation and testing. There are two tests conducted during the project execution. The first one is Vicker's microhardness test which is carried out to assess the effect of FSP on mechanical properties of the Al-FA-Gr composites. The microhardness behaviour is tested by using AFFRI 251.VRSD (D Series) with the compliance of ASTM E-384; Standard test method for metallic materials using an applied force from 1kgf to 120kgf. The tester consists of a small pyramid shaped diamond indenter with an apical angle of 136°, which is pressed into the test sample at a predetermined load. An optimum load of 1000 g and dwell time of 15 s are applied to run the testing.  $D_1$  and  $D_2$  values are captured and resulted to HV values of the samples.

For the next steps, the composites are etched with Keller's etchant that is made up of several types of liquid to reveal the grain boundaries. Distilled water, nitric acid, hydrochloric acid and hydrofluoric acid are measured to 190 ml, 5 ml, 3 ml and 2 ml respectively. The samples are then immersed in the fresh etchant for 10 secs and rinsed with ethanol and tap water. Prepared samples are examined with microstructural characterization by using Optical Microscopy that used LAS V4.5 software. Focus knob is moved until the sample's microstructure comes into focus. Then, the condenser and light intensity are adjusted for the greatest amount of light to capture the images. The investigation is focused more on the grains, grain boundaries and interfaces between aluminium matrix and FA-Gr reinforcements.

## **3.2 Sampling Specifications**

### **3.2.1 Metal Matrix**

- *Aluminum Plates AA-7075-T651*

Since there were two parameters (hybrid composition and volume percentage) with three categories each, The sample size required for this project is  $3^2$ , totalling up to 9 aluminum samples of the same size. Commercially available, three pure aluminum plates (AA7075-T651) are prepared as substrates with dimensions of 100 mm × 150 mm × 6 mm as shown in Figure 3.4.

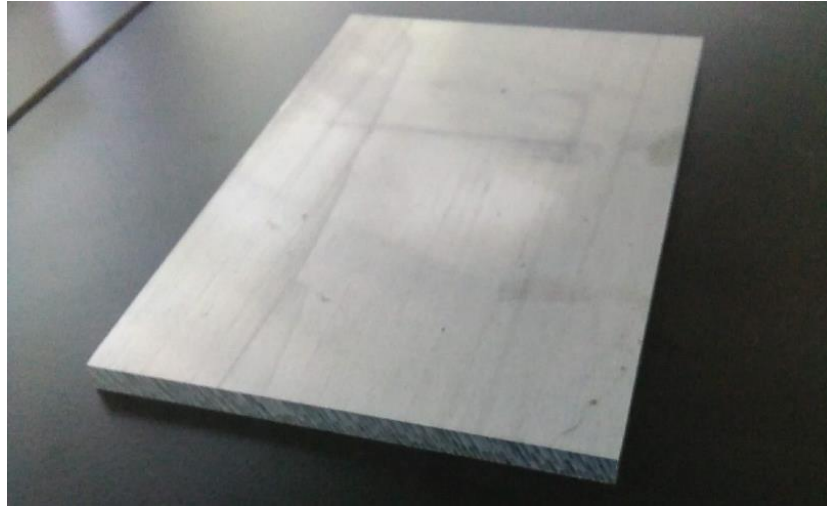


FIGURE 3.4 : 7075 Aluminium plate

### 3.2.2 Reinforcement Powders

Two types of powders are needed for dispersion of particle reinforcements to produce a hybrid composites.

- *Fly Ash Micro powder*  
Purity : 99 %  
APS : 40 – 50  $\mu\text{m}$
- *Nano Graphite powder*  
Purity : 99.9 %  
Thickness : < 40 nm  
Flake diameter : 3 – 6  $\mu\text{m}$

### 3.3 Equipments and Consumables

#### 3.3.1 Vertical Turret Milling machine

Vertical milling machine as shown in Figure 3.5 is a precision tool used for forming and fabricating by removing stock from metallic workpieces. For instance, drilling holes on plates. The High Speed Steel Aluminium (HSSAL) end mill that has three flutes and 3 mm mill diameter as in Figure 3.6 is selected.



FIGURE 3.5 : Vertical Turret Milling Machine



FIGURE 3.6 : End mill

#### 3.3.2 Turbula Mixer

Figure 3.7 portrays a mixer that is used for homogeneous mixing of powdery materials of different weights and particle sizes. The container is set up as a three-dimensional motion (a combination of rotation, translation, and inversion).



FIGURE 3.7 : Turbula Mixer and Glass Jar

### 3.3.3 Weighing Balance

Analytical balance as in Figure 3.8 is known as a very accurate device designed for measuring weight of small mass in sub-milligram range. Reinforcement powders are handled with spatula and weighed powders are stored in containers as labelled in Figure 3.9.

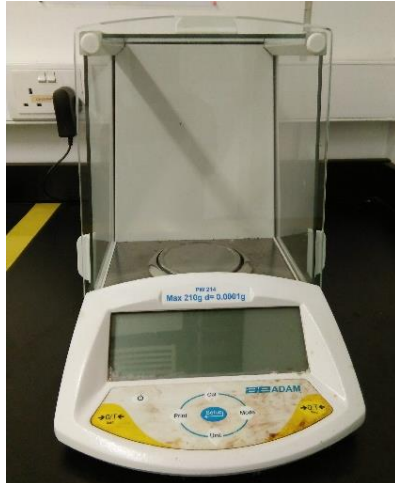


FIGURE 3.8 : Weighing Balance



FIGURE 3.9 : Containers

### 3.3.4 Friction Stir Welding machine

Since FSP has the same working principle as FSW, it is effective to use the FSW machine as shown in Figure 3.10 below. The tool used for FSP process is made up of H13 steel with straight cylindrical pin profile. The dimensions of the tool are 4.5 mm pin length, 20 mm shoulder diameter and 6 mm pin diameter. Refer to Figure 3.11 for the pin profile.



FIGURE 3.10 : FSW Machine



FIGURE 3.11 : Pin Profile

### 3.3.5 Electrical Discharge Machine

Machine as displayed in Figure 3.12 is used for a controlled metal-removal process called EDM. The machine applies electric spark erosion to cut the metal and it works in the water. This type of machining is able to cut extremely hard material to very close tolerances. To wire cut the samples, common brass EDM wire that made up of copper with additional zinc is used.



FIGURE 3.12 : Electro Discharge Machining

### 3.3.6 Automatic Mounting Press

Figure 3.13 shows the mounting press machine which produces uniform-sized specimens that can be handled easily. The specimens are mounted under the presence of pressure and heat. In order to complete a cycle, the samples undergone four steps which are pre-heating, pressurize, cooling and de-pressurize. Phenolics granules in Figure 3.14 are mounted as the compression resins and release agent is coated on the selected surfaces that being tested.



FIGURE 3.13 : Mounting Press Machine

FIGURE 3.14 : Phenolics Granules

### 3.3.7 Grinder Polisher

Grinding and polishing machine as in Figure 3.15 aims to produce a final polished-without-deformation samples which prepared for analysis. For grinding process, it needs Silicon Carbide (SiC) papers with different grit size and water as lubricants. While for polishing step, velvet cloth is used as a replacement for the SiC paper and impregnated with diamond suspension (metaDi fluid). Other material needed to polish the samples include diamond polishing compound (metaDi II) as shown in Figure 3.16.



FIGURE 3.15 : Grinder Polisher



FIGURE 3.16 : Diamond Paste

### 3.3.8 Microhardness Testing Machine

Figure 3.17 shows the Vicker's microhardness tester that applies the system of optical measurement. It specifies a range of light loads using a diamond indenter to make an indentation which is then measured and converted to a hardness value.

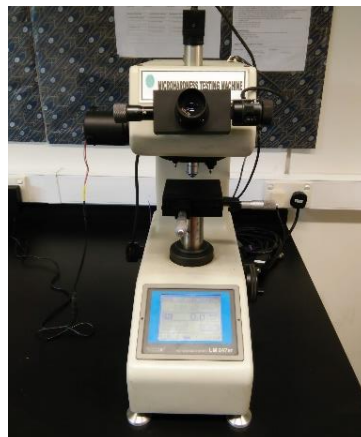


FIGURE 3.17 : Vicker's Microhardness Testing Machine

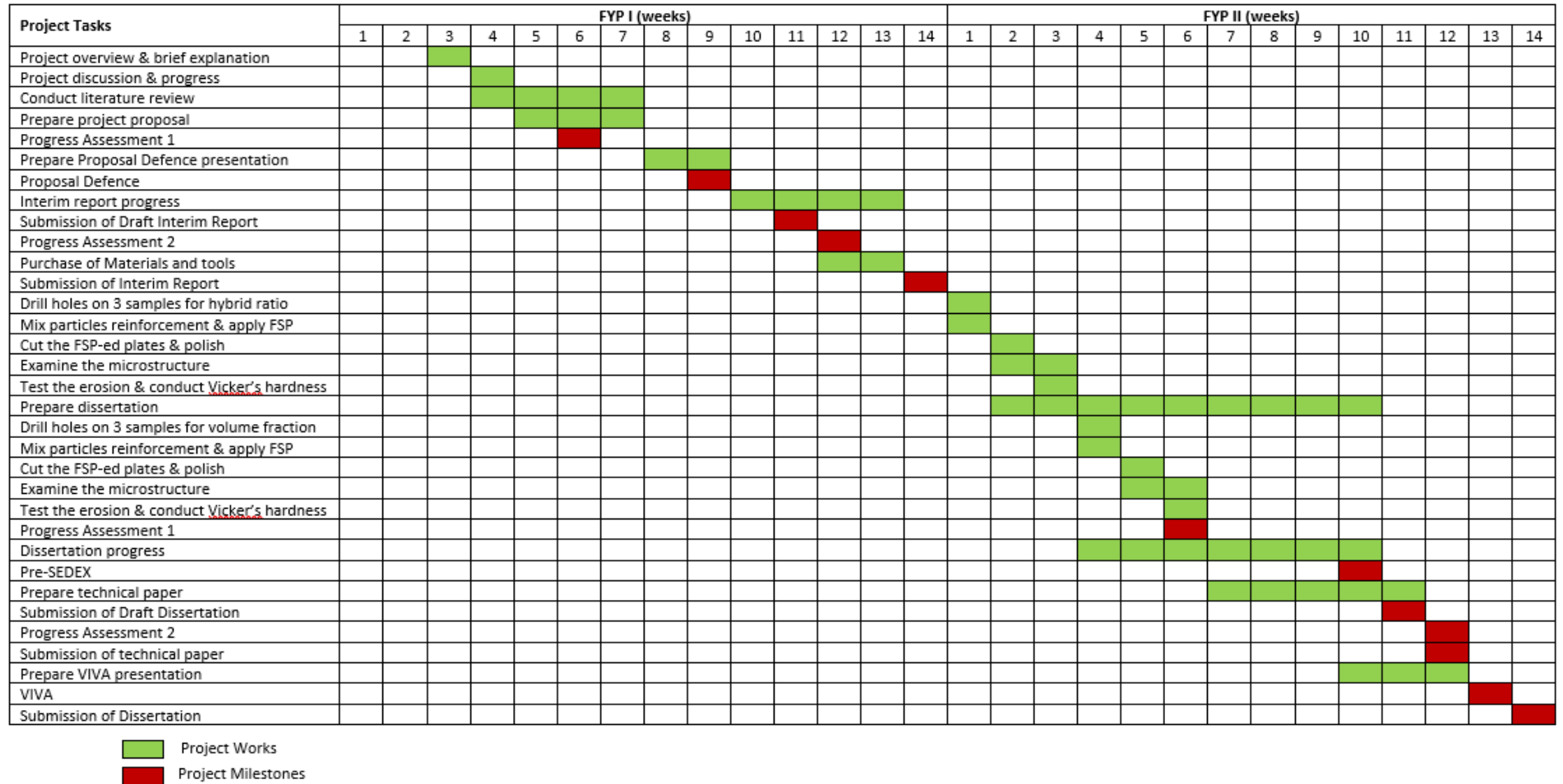
### 3.3.9 Optical Microscope

Basic functions of Optical Microscope as displayed in Figure 3.18 are generating magnified images and illuminating a sample. The observation optical system projects a sample through an optical system and guides a projection image to the eye or the pickup device. When light source emits light, illumination optical system collects it and leads the light to the sample to illuminate it.



FIGURE 3.18 : Optical Microscope

### 3.4 Project Activities and Milestone



## CHAPTER 4

### RESULTS AND DISCUSSIONS

#### 4.1 Microhardness

Hardness is not a fundamental physical property but a characteristic of a material. The definition of hardness is resistance to indentation, and it is determined by measuring the permanent depth of the indentation. The measured base alloy is about 85 HV. All composites show increment and improvement in the hardness properties.

##### 4.1.1 Data Tabulation

The results of indentation size and hardness value obtained from Vicker's hardness test that have been carried out are collected in Table 4.1 until Table 4.10. While summary of the test is tabulated as in Table 4.11. The results are then analysed by using ANOVA Analysis method and illustrated by plots and a contour graph.

TABLE 4.1 : Run 1 Hardness Test Results

Test	1	2	3	4	5	average
D1	143.19	139.91	130.53	134.02	150.64	139.66
D2	144.16	141.43	131.98	134.77	149.34	140.34
HV	89.80	93.70	107.60	102.70	82.40	98.98

TABLE 4.2 : Run 2 Hardness Test Results

Test	1	2	3	4	5	average
D1	140.75	133.65	137.71	139.93	143.37	138.97
D2	145.35	133.63	137.71	139.39	147.50	140.72
HV	90.60	103.80	99.40	95.10	87.70	96.63

TABLE 4.3 : Run 3 Hardness Test Results

Test	1	2	3	4	5	average
D1	146.05	136.19	131.09	130.16	140.87	136.87
D2	145.77	137.43	132.63	130.16	140.87	137.37
HV	87.10	99.10	106.70	108.50	93.50	100.56

TABLE 4.4 : Run 4 Hardness Test Results

<b>Test</b>	<b>1</b>	<b>2</b>	<b>3</b>	<b>4</b>	<b>5</b>	<b>average</b>
D1	135.65	125.29	123.34	146.50	129.61	132.08
D2	134.76	124.25	124.50	146.50	132.07	132.42
HV	101.40	119.10	120.80	86.60	108.30	102.65

TABLE 4.5 : Run 5 Hardness Test Results

<b>Test</b>	<b>1</b>	<b>2</b>	<b>3</b>	<b>4</b>	<b>5</b>	<b>average</b>
D1	142.34	134.20	136.47	143.79	143.06	139.97
D2	146.33	134.81	136.64	143.79	143.06	140.93
HV	89.00	102.50	99.40	91.40	88.50	95.12

TABLE 4.6 : Run 6 Hardness Test Results

<b>Test</b>	<b>1</b>	<b>2</b>	<b>3</b>	<b>4</b>	<b>5</b>	<b>average</b>
D1	146.84	124.79	123.65	136.86	144.66	135.36
D2	146.84	124.79	125.39	136.07	145.05	135.63
HV	87.40	117.20	119.60	99.60	88.40	101.95

TABLE 4.7 : Run 7 Hardness Test Results

<b>Test</b>	<b>1</b>	<b>2</b>	<b>3</b>	<b>4</b>	<b>5</b>	<b>average</b>
D1	141.73	129.98	135.12	127.42	150.74	137.00
D2	149.23	133.82	136.07	127.42	149.53	139.21
HV	87.60	106.60	100.90	114.70	82.30	100.02

TABLE 4.8 : Run 8 Hardness Test Results

<b>Test</b>	<b>1</b>	<b>2</b>	<b>3</b>	<b>4</b>	<b>5</b>	<b>average</b>
D1	142.17	143.74	132.83	142.57	149.51	142.16
D2	142.17	144.94	133.41	142.57	149.51	142.52
HV	88.80	89.00	104.60	92.00	84.80	93.76

TABLE 4.9 : Run 9 Hardness Test Results

<b>Test</b>	<b>1</b>	<b>2</b>	<b>3</b>	<b>4</b>	<b>5</b>	<b>average</b>
D1	137.51	134.36	122.50	133.15	143.83	134.27
D2	136.52	134.36	123.98	134.12	150.49	135.89
HV	98.80	102.50	122.10	103.80	85.60	102.56

TABLE 4.10 : Run 10 Hardness Test Results

Test	1	2	3	4	5	average
D1	143.19	139.91	131.53	134.02	150.64	139.66
D2	144.19	141.53	131.98	133.77	150.34	140.34
HV	89.80	93.80	107.80	103.70	82.40	99.10

TABLE 4.11 : Hardness Test Results Summary

Run no.	Hybrid ratio (FA : Gr)	Volume percentage (%)	Hardness value (HV)
1	60 : 40	4	98.98
2	60 : 40	12	96.63
3	60 : 40	8	100.56
4	90 : 10	4	102.65
5	90 : 10	12	95.12
6	90 : 10	8	101.95
7	75 : 25	4	100.02
8	75 : 25	12	93.76
9	75 : 25	8	102.56
10	75 : 25	8	99.10

As shown in table above, run 10 might be the same as run 9 but with different value. Basically, run 10 is the replication of run 9. This is because run 10 which called as center point run, is needed for later analysis. It is a condition of central composite design in the statistical approach, RSM.

#### 4.1.2 ANOVA Analysis

ANOVA method of analysis; a variance analysis used to evaluate whether statistically significant discrepancies exist between the means of three or more separate (unrelated) groups. Results calculated from ANOVA Analysis are summarized and tabulated as per Table 4.12 and 4.13.

TABLE 4.12 : ANOVA Analysis Input

Response	Name	Obs	Analysis	Min	Max	Mean	Std dev	Ratio	Model
R1	HV	10	Polynomial	93.76	102.65	99.1335	3.09389	1.09482	Quadratic

TABLE 4.13 : ANOVA Analysis Summary

ANOVA for Response Surface Quadratic model						
Source	Sum of Squares	df	Mean Square	F Value	p-value Prob > F	
Model	78.95	5	15.79	8.77	0.0281	significant
A (HR)	2.09	1	2.09	1.16	0.3415	
B (Vol%)	43.42	1	43.42	24.12	0.0080	
AB	6.71	1	6.71	3.73	0.1258	
A <sup>2</sup>	2.40	1	2.40	1.33	0.3123	
B <sup>2</sup>	26.23	1	26.23	14.57	0.0188	
Residual	7.20	4	1.80			
Lack of Fit	1.22	3	0.41	0.068	0.9689	not significant
Pure Error	5.99	1	5.99			
Cor Total	86.15	9				

In order to find the effectiveness of both parameters towards the project, Anova Analysis has been conducted. The parameters are represented by A and B for hybrid ratio and volume percentage, respectively. In this analysis, both P-value and F-value tells about the significance of parameters used. A parameter can be effective if there is a large difference between both values. To achieve that, the P-value must be smaller while F-value is higher. From the findings, F-value of model which is 8.77 implies that the model is significant. There is only a 2.81% chance that an F-value this large could occur due to noise. For a model term to be indicated as significant, the P-value must be less than 0.0500. As in this case, B and B<sup>2</sup> shows lower value than 0.0500 which are 0.0080 and 0.0188. By means, volume percentage factor is a significant model term.

P-value that is greater than 0.1000 indicates that the model terms are not significant. This can be seen from value generated for hybrid ratio, A and A<sup>2</sup> which are 0.3415 and 0.3123, respectively. When there are several meaningless terms of the model (not counting those needed to maintain hierarchy), reduction of the model will increase efficacy. Comparing to these two parameters, p-value of volume percentage is way smaller than hybrid ratio which is 0.0080 : 0.3415. The huge difference between p-value and f-value is also owned by volume percentage. This indicates that volume percentage is more effective and significant compared to hybrid ratio.

Next, Lack of fit is the indication of fitting curve of the data with quadratic behaviour. "Lack of Fit F-value" of 0.068 implies the Lack of Fit is not significant relative to the pure error. There is a 96.89% chance that a "Lack of Fit F-value" this large could occur due to noise. P-value of this model is almost reaching to 1 where 1 is the perfect fit. Hence, this proves that non-significant lack of fit is good and a good fit portrays a good model.

The data and results from hardness test and anova analysis are then extracted in a fit below. From the data tabulated, the highest HV is at 90:10 hybrid ratio with value of 102.65. Unfortunately, there is no improvement shown when volume percentage is increasing. Eventhough 60:40 shows the improvement, it is not that impressive compared to 75:25. Since data at hybrid ratio of 75:25 shows significance, thus it has become the interest and portrayed as shown in Figure 4.1. The largest improvement can be seen with increment of 2.54 from 4% to 8% volume percentage. Then, increasing volume of reinforcement only decrease the hardness.

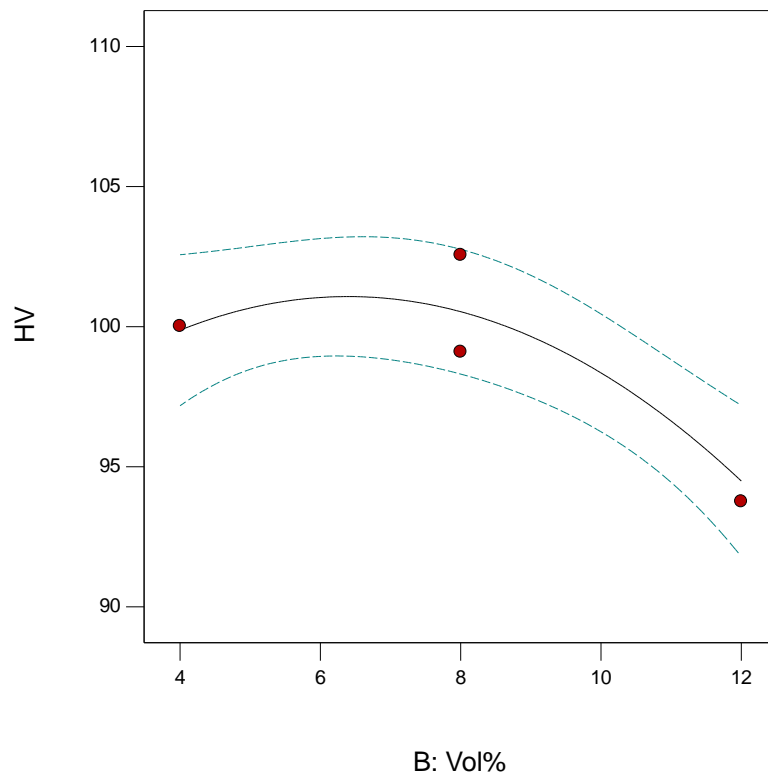


FIGURE 4.1 : Graph of Volume Percentage at 75:25 Hybrid Ratio (vol%) vs Microhardness (HV)

As for volume percentage, the most significant is at 8% reinforcement particles since decrease in hardness is seen afterward. The data are extracted in the fit as displayed in Figure 4.2. The trend line can be interpreted as linear. Increasing hybrid ratio affects in increase of the hardness value. This means that hardness is higher with greater fly ash content. It is also supported with soft and lubricative in nature of graphite characteristics.

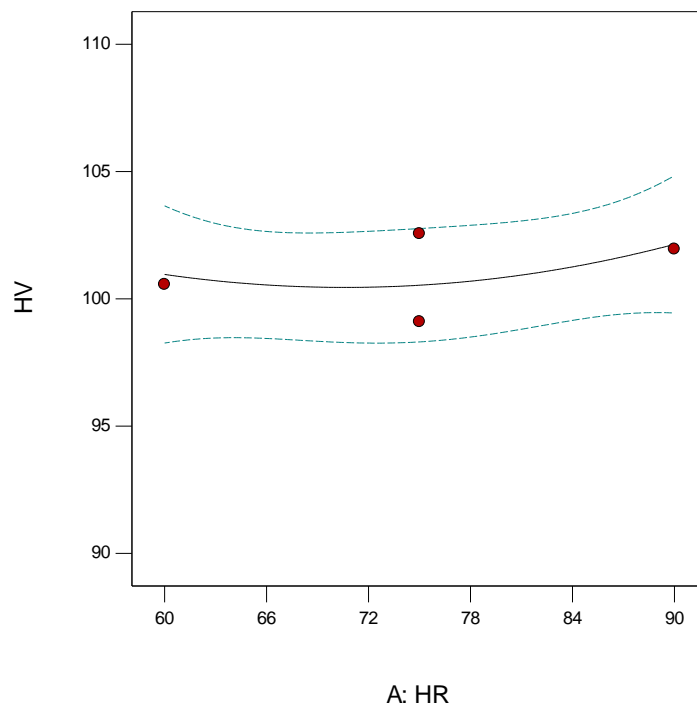


FIGURE 4.2 : Graph of Hybrid Ratio at 8% Volume Percentage (HR) vs Microhardness (HV)

### 4.1.3 Contour Graph

From the contour graph generated by Design Expert 10, several important data can be highlighted. The graph presents HV for both parameters investigated in the project. The highest HV of 102 is at the red area. The black lines on the graph are called contour lines. These lines are used to present different ranges of HV. Based on that, optimum value for both parameters can be obtained as shown in Figure 4.3. Hence, optimum hybrid ratio for the project is 84 – 90 % fly ash content with 10 – 15 % graphite. While the optimum volume percentage is 4% to 8% fly ash-graphite reinforcement particles.

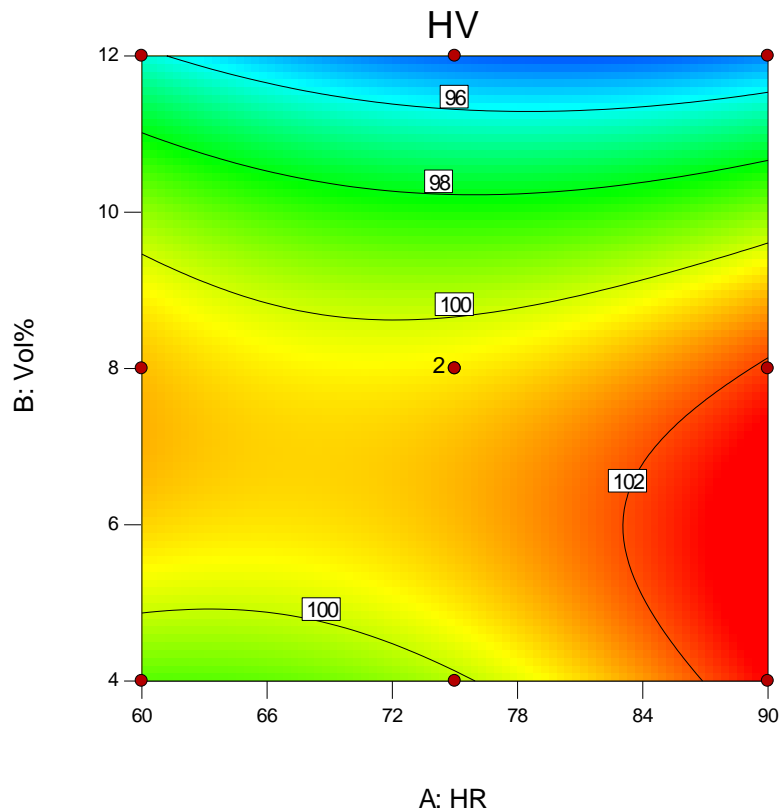


FIGURE 4.3 : Contour Graph of Hybrid Ratio and Volume Percentage vs Microhardness

## 4.2 Microstructure

Microstructure characterization for this project is also conducted by using Optical Microscope to see the interfaces between aluminium matrix and reinforcement particles which are fly ash and graphite. Besides, investigation is also made to check on the grain and grain boundaries of the composites. The magnification used for the characterization are 50X, 100X and 500X. Since run 4 (90:10 hybrid ratio with 4% vol%) has the highest hardness value and run 8 (75:25 hybrid ratio with 12% vol%) has the lowest, microstructure of both composites came into consideration and investigated.

### 4.2.1 Data Collections and Analysis of Run 4 Composites

The microstructures for the highest hardness composites produced which is run 4 are illustrated as in Figure 4.4 until 4.6.

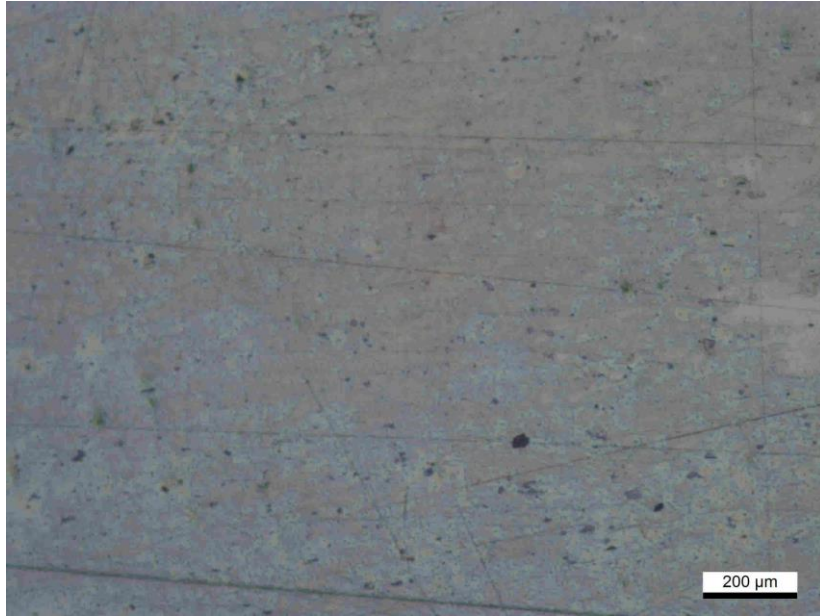


FIGURE 4.4 : 50X Magnification of Run 4 Composites

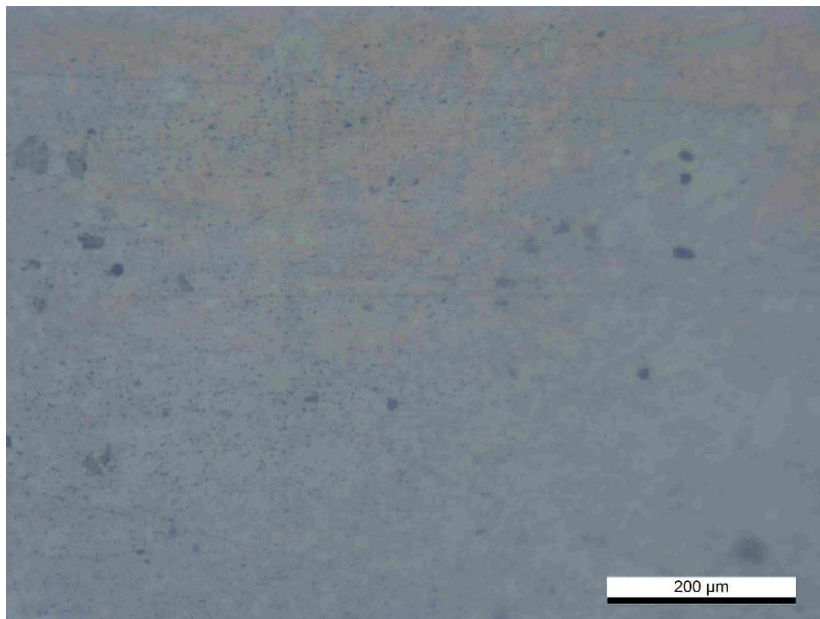


FIGURE 4.5 : 100X Magnification of Run 4 Composites

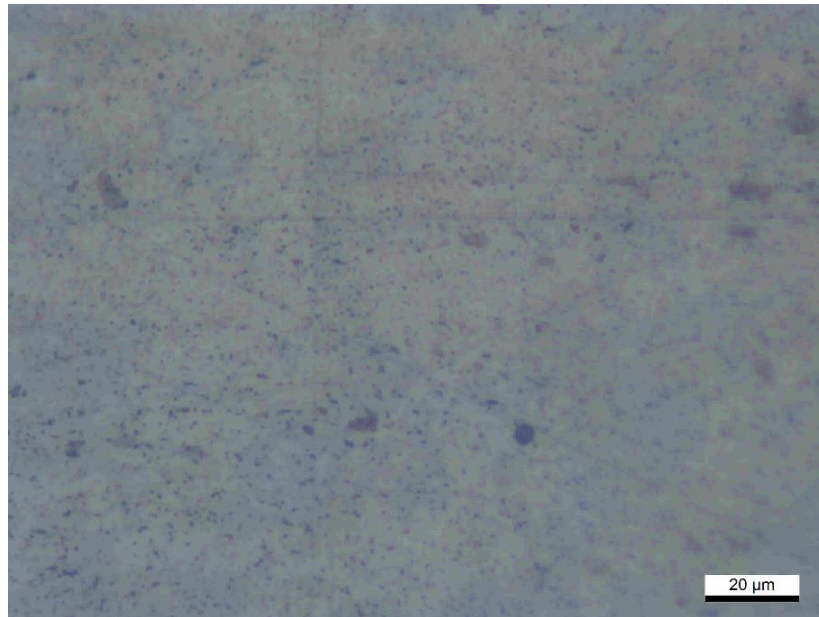


FIGURE 4.6 : 500X Magnification of Run 4 Composites

From the microstructures of run 4, second phase particles of fly ash and graphite is seen to be homogenously distributed even the reinforcements in the sample that can still be seen in the image captured have fragmented into irregular sizes caused by the intense plasticization. Since the stirring action of rotational speed during the FSP process is high, the material movement allowed the dispersal of FA/Gr powders well and has provided ample chances to encapsulate the graphitic layers around the FA particles. The exfoliated graphitic layers served as a link between the matrix and FA/Gr reinforcements and thus led to the greater interfacial bonding.

Furthermore, increasing in filler loading which is the fly ash, also contributed to the increase of the interfacial area between filler and aluminium as well as reduce of free motion and avoid the deformation of matrix. As the interfacial area increased, it increases the worsening bonding between reinforcement and matrix which then became one of the factor the high value of hardness obtained from the experiment. Filler loading increment also shown a tendency to increase the stiffness, brittleness and rigidity of the AA/FA/Gr composites since there are presence of voids which obstruct the stress propagation.

The dispersion of the FA/Gr reinforcement particles in the base alloy has influenced the resulting grain size achieved within the composites. Due to the presence of reinforcements, the grain growth in processed composites is mainly regulated by the pinning effect. The increase in hardness is related to the strengthening of the grain size due to the restriction of grain growth by pinning effects of reinforcements. Hence, more refined grain structure is finally obtained in surface composites induced by reinforcement encapsulation during extreme plasticisation.

#### **4.2.2 Data Collections and Analysis of Run 8 Composites**

The microstructures for the lowest hardness composites produced which is run 8 are illustrated as in Figure 4.7 until 4.9.

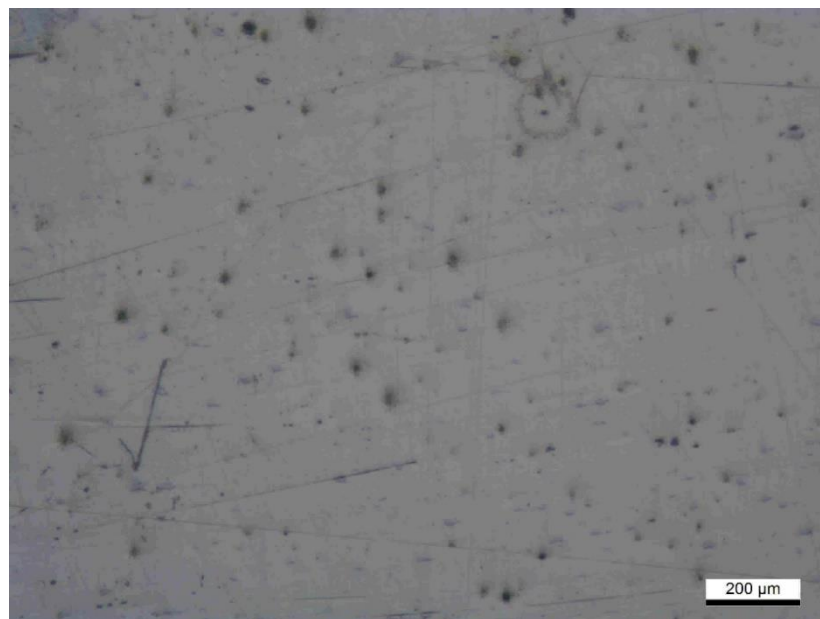


**FIGURE 4.7 : 50X Magnification of Run 8 Composites**

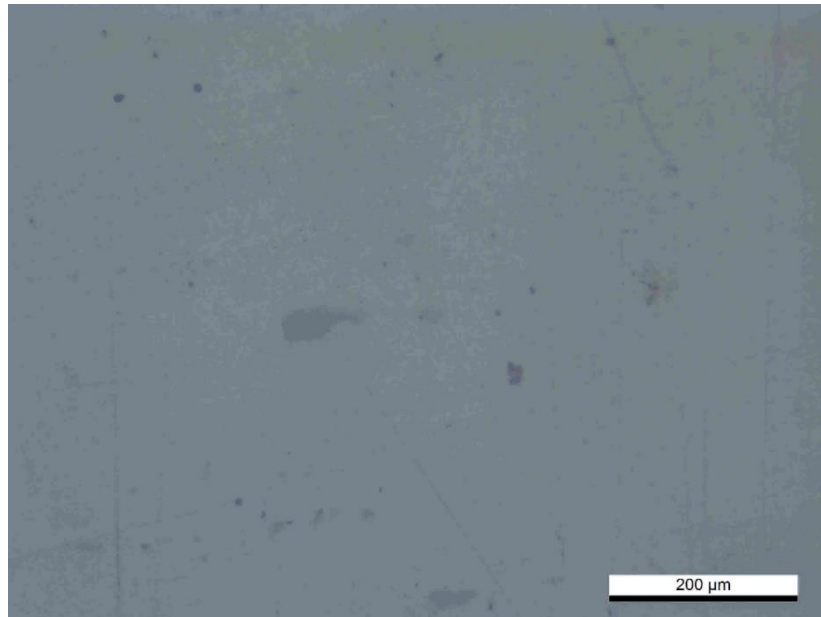


FIGURE 4.8 : 100X Magnification of Run 8 Composites

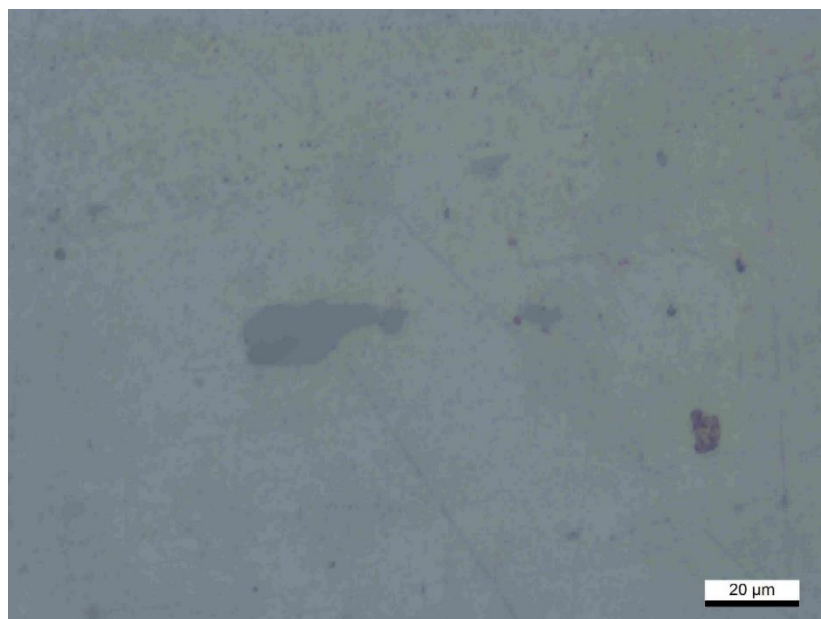


FIGURE 4.9 : 500X Magnification of Run 8 Composites

From Figure 4.7 until 4.9, the microstructure of the lowest hardness composites can be seen to have homogeneity in particles distribution. Unfortunately, there are huge reinforcements particles clearly shown on the magnifications of surface composites. Due to intense plasticization, graphite flakes turned into are multilayered graphene and fly ash particles get fragmented

into uneven sizes. Due to the breakdown of precipitates during extremely super plastic deformation, the FSP process tended to reduce the hardness of this composite. Besides, the interfaces between fly ash-graphite and aluminium matrix is lower compared to run 4 composites. Poor interfacial bonding is then caused partially separated micro-spaced between filler particles and the aluminum matrix. The 12% volume percentage of reinforcement in the composite has exceeded the capacity of aluminium matrix to bind and transferred in between all the particles.

Microhardness has been regulated mainly by two mechanisms in the composites which are retention of endogenous precipitates within base alloy as well as strengthening of uniform grain size as a result of pinning effect. The decrease in dislocation densities due to discrepancy of reinforcements thermal coefficients and base alloy also led to the decrease in the microhardness of the resulting composites. Next, the bigger grains size in run 8 composite has led to the lower microhardness results since lower restriction of abnormal grain growth obtained from the characterization.

## CHAPTER 5

### CONCLUSION AND FUTURE WORK

The contingency of mechanical property over the hybrid ratio and volume percentage is investigated on fly ash-graphite reinforced aluminium alloy composite material in the present work. The composites are fabricated by the implementation of FSP technology. The mechanical tests; Vicker's microhardness, are conducted as per the relevant ASTM standards. ANOVA analysis is then carried out to determine the significance of both parameters on composites' microhardness. The reasons of contribution to the highest and lowest hardness value obtained validated using the optical microscopy characterization. Based on the conducted experiment, the conclusion of response variation with regards to the microstructural observations have been made.

Objectives have been achieved since all composites produced owned higher microhardness rather than base alloy itself. For hybrid ratio parameter investigation, there was nonlinear relationship where the hardness increased steadily to the increase of fly ash content from 60:40 to 90:10. The optimum hybrid ratio of the project is found to be ranging from 84:16 to 90:10.

While for volume percentage, hardness is increased with the increment of reinforcements particles from 4% to 8% with great and significant improvement. But, hardness is then rapidly decrease or level out towards a minimum after 8% volume percentage is applied. This can be seen from 12% volume percentage that has the lowest hardness value. The optimal reinforcements' volume percentage obtained from the experiment was ranging from 4% to 8%.

Microhardness is the best on sample with hybrid Fly Ash – Graphite ratio of 90:10. It showed that the use of agrowastes such as fly ash in this project, enhanced microhardness and microstructure due to its high strength property. ANOVA analysis indicated that between those two parameters investigated, volume percentage attribution is more significant to the hardness behaviour of AA/FA/Gr composites. The mechanical properties is improved effectively after FSP due to the microstructural improvement.

Optical microscopy images of the microstructures validate the experimental results and proves the fact that FSPed samples achieved an improvement in the homogeneity of particle distribution. A single pass of FSP was enough to break the particle segregation from the grain boundaries and improve the distribution. The greater interfacial bonding between the reinforcement and matrix, finer average grains size and higher dislocation density obtained from the composite fabrication are contributed to the significant enhancement of the hardness behaviour.

Lesson learned from this project, it is recommended to reduce errors such as human error during the experimental work in the future. Other mechanical tests can be conducted for these samples for instance wear resistance and tensile strength. Parameters such as rotational and transverse speed are also encouraged to be studied since they may have greater improvement on hardness and other tribological and mechanical characteristics of fabricated composites.

## REFERENCES

- [1] R. S. Mishra, Z. Y. Ma and I. Charit, "Friction stir processing: a novel technique for fabrication of surface," *Materials Science and Engineering : A*, vol. 341, no. 1-2, pp. 307-310, 2003.
- [2] Y. Wang and R. S. Mishra, "Finite element simulation of selective superplastic forming of friction stir processed 7075 Al alloy," *Materials Science and Engineering A*, vol. 463, no. 1-2, pp. 245-248, 2007.
- [3] W. M. Thomas, K. I. Johnson and C. S. Wiesner, "FRICTION STIR WELDING - RECENT DEVELOPMENTS IN TOOL AND PROCESS TECHNOLOGIES," *Advanced Engineering Materials*, vol. 5, no. 7, pp. 485-490, 2003.
- [4] S. X. McFadden, A. P. Zhilyaev, R. S. Mishra and A. K. Mukherjee, *Materials Letters*, vol. 45, no. 6, pp. 345-349, 2000.
- [5] G. V. N. B. Prabhakar, K. N. Ravi and S. B. Ratna, "Surface metal matrix composites of Al5083 - fly ash produced by friction stir processing," *Materials Today: Proceedings 5*, vol. 5, no. 2, p. 8391–8397, 2018.
- [6] W. F. Smith and J. Hashemi, *Foundations of Materials Science and Engineering*, McGraw-Hill, 2003.
- [7] R. Nelson, I. Dinaharan and S. J. Vijay, "Design and development of Fly ash reinforced aluminium matrix composite using friction stir process (FSP)," in *Institute of Electrical and Electronics Engineering*, Nagercoil, India, 2013.
- [8] W. D. Callister Jr and D. G. Rethwisch, *Materials Science and Engineering: An Introduction*, vol. Eight Edition, United States of America: John Wiley & Sons, Inc, 2010.
- [9] L. W. Davis, "How Metal Matrix Composites Are Made," *Fiber-Strengthened Metallic Composites*, pp. 69-90, 1967.
- [10] A. Thirumoorthy, T. V. Arjunan and K. K. L. Senthil, "Latest Research Development in Aluminum Matrix with Particulate," *Materials Today: Proceedings*, vol. 5, no. 1, pp. 1657-1665, 2018.
- [11] K. D. Basham, M. Clark, T. France and P. Harrison, "ADDING FLY ASH TO CONCRETE MIXES FOR FLOOR CONSTRUCTION," *Concrete Construction*, 29 November 2007. [Online]. Available: <https://www.concreteconstruction.net/how-to/construction/adding-fly-ash-to->

concrete-mixes-for-floor-construction\_o. [Accessed November 2019].

- [12] A. Tangarasu, N. Murugan, I. Dinaaran and S. J. Vijay, Synthesis and characterization of titanium carbide particulate reinforced AA6082 aluminium alloy composites via friction stir processing, 2014.
- [13] E. T. Akinlabi, R. M. Mahamood, S. A. Akinlabi and E. Ogunmuyiwa, Processing Parameters Influence on Wear Resistance Behaviour of Friction Stir Processed Al-TiC Composites, 2014.
- [14] V. Sharma, U. Prakash and K. B. V. Manoj, "Surface Composites by Friction Stir Processing : A review," *Journal of Materials Processing Technology*, vol. 224, pp. 117-134, 2015.
- [15] H. Sarmadi, A. H. Kokabi and S. M. Seyed Reihani, "Friction and wear performance of copper-graphite surface composites," *Wear*, vol. 304, no. 1-2, pp. 1-12, 2013.
- [16] Y. X. Gan, D. Solomon and M. Reinbolt, "Friction Stir Processing of Particle Reinforced Composite," *Materials*, vol. 3, no. 1, pp. 329-350, 2010.
- [17] M. S. Węglowski, "Friction stir processing – State of the art," *Archives of Civil and Mechanical Engineering*, vol. 18, no. 1, pp. 114-129, 2018.
- [18] T. Hirata, T. Morishige, M. Tsujikawa and K. Higashi, Influence of alloying elements on grain sizes in friction stir processed pure aluminium and aluminium alloys, 2011.
- [19] A. P. Namdev, R. P. Srinivasa, M. Othman and S. L. Abdul Munir Hidayat, "Optimization of Friction Stir Process Parameters for Enhancement in Surface Properties of Al 7075-SiC/Gr Hybrid Surface Composites," *Coatings*, vol. 9, no. 830, December 2019.
- [20] O. M. Ikumapayi, E. T. Akinlabi, S. K. Pal and J. D. Majumdar, "A survey on reinforcements used in friction stir processing of aluminum metal matrix and hybrid composites," in *2nd International Conference on Sustainable Materials Processing and Manufacturing*, 2019.
- [21] J. Shan, "Laser welding of magnesium alloys," in *Welding and Joining of Magnesium Alloys*, UK, Woodhead Publishing Limited, 2010, pp. 306 - 350.